Optical conductivity of a strong-coupling Fröhlich polaron

S. N. Klimin* and J. T. Devreese†

Theorie van Kwantumsystemen en Complexe Systemen, Universiteit Antwerpen, Universiteitsplein 1, B-2610 Antwerpen, Belgium

(Received 12 June 2013; revised manuscript received 19 November 2013; published 3 January 2014)

The polaron optical conductivity at zero temperature is derived within the strong-coupling approximation accounting for internal nonadiabaticity. The polaron optical conductivity spectrum is provided by the multiphonon optical transitions. The polaron optical conductivity spectra calculated within our analytic strong-coupling approach and the numerically accurate diagrammatic quantum Monte Carlo (DQMC) data are in a good agreement with each other at large $\alpha \gtrsim 9$.

DOI: 10.1103/PhysRevB.89.035201 PACS number(s): 71.38.Fp, 02.70.Ss, 78.30.−j

I. INTRODUCTION

Polaron is one of the most known problems of the quantum field theory, which seems to be simple, but it is not yet solved analytically exactly, despite many-year attempts to find a solution.[1] Particularly, the optical response of a polaron attracted attention for years because of experimentally observed manifestations of polaronlike behavior of the midinfrared optical absorption of polar crystals and high-T_c superconductors.[2–7] The problem of the polaron optical response is important also for theorists, because it is a field for testing various theoretical techniques, such as perturbation approach and canonical transformations at weak coupling, the adiabatic approximation at strong coupling, variational all-coupling methods involving path integral formalism of quantum mechanics and quantum Monte Carlo calculations.

In the literature, several theoretical approaches for the polaron optical conductivity are available, depending on the polaron coupling strength. In the regime of weak coupling, the optical absorption of a polaron in the lowest order on the polaron coupling constant α was calculated using, e.g., Green's function method[8] and the Low–Lee–Pines formalism.[9] The exact results for the free-polaron optical absorption up to order α^2 Ref. 10 were obtained by a systematic perturbation expansion of the current-current correlation function. In the opposite, strong-coupling regime, the polaron optical conductivity was calculated taking into account one-phonon[11] and two-phonon[12] transitions from the polaron ground state to the polaron relaxed excited state (RES).

Within the alternative methods for the strong-coupling polaron optical conductivity developed in Refs. 13 and 14, the polaron optical response is assumed due to transitions to continuum polaron states, i.e., the polaron dissociation. However, this assumption is in contradiction with the fact established by Pekar[15] that the oscillator strengths of the transition of an electron from the polaron ground state to the continuum part of the energy spectrum is very small with respect to the oscillator strength of the transition between the ground and first excited state, especially at strong coupling. Therefore it seems that the approach of Ref. 13 captures only a relatively small part of the strong-coupling polaron optical conductivity.

Using the path integral response formalism, the impedance function of an all-coupling polaron was calculated by Feynman *et al.*[16] on the basis of the Feynman polaron model.[17] Developing further the approach of Ref. 16, the optical conductivity was calculated within the path-integral formalism.[18,19] The analytic treatment[18] was intended to be valid at all coupling strengths. However, as established in Ref. 18, the linewidth of the obtained spectra[18] is unreliably small for $\alpha \gtrsim 7$.

Recently, the diagrammatic Quantum Monte Carlo (DQMC) numerical method has been developed,[20,21] which provides accurate results for the polaron characteristics in all coupling regimes. The DQMC has been also applied to the optical conductivity of small (Holstein) polaron, compared with the analytic method of the momentum average approximation.[22,23] The large-polaron optical conductivity calculated by DQMC exhibits a broad spectrum in the strong-coupling regime, contrary to Ref. 18. Nevertheless, as seen from Fig. 1, the position of the peak attributed to RES in Ref. 18 is close to the maximum of the polaron optical conductivity band calculated using DQMC up to very large values of α.

This stimulated further efforts on analytic approaches to the polaron optical conductivity. In Ref. 24, the extension of the method of Ref. 18 accounting for the polaron damping (for the polaron coupling constant $\alpha \lesssim 8$) and the asymptotic strong-coupling approach using the Franck–Condon (FC) picture for the optical conductivity (for $\alpha \gtrsim 8$) have given reasonable results for the polaron optical conductivity at all values of α. The concept of the RES and FC polaron states played a key role in the understanding of the mechanism of the polaron optical conductivity.[11,18]

An improvement of the path-integral approach[18] performed in Ref. 24 using the extended memory-function formalism (MFF) gives a good agreement with DQMC for weak and intermediate coupling strengths. In the strong-coupling limit, in Ref. 24, the Franck-Condon (FC) approximation is used. That calculation is not exact in the strong-coupling limit because of a parabolic approximation[25] for the adiabatic potential. However, it provides a good (at least qualitatively) agreement of the analytically determined strong-coupling polaron optical conductivity with the DQMC data. The extended MFF and the FC approximations partly overlap in the range $\alpha \sim 8$, showing close results for the optical-conductivity spectra. However, a unified approach describing the polaron optical conductivity for all α is not yet found. Moreover, a deeper study of the polaron optical response in the strong-coupling regime represents an interest because of (1) a possibility of use of more accurate strong-coupling trial polaron wave

 ©2014 American Physical Society

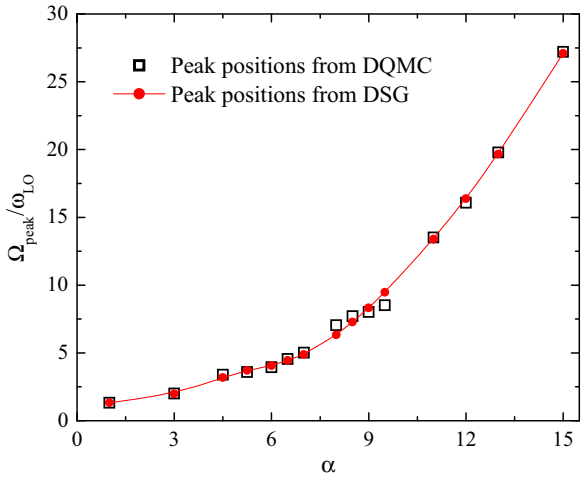

FIG. 1. (Color online) Frequency of the main peak in the optical conductivity spectra calculated within the model of Ref. 18 (dots) and the main-peak energy extracted from the DQMC data[21,24] (squares).

functions and energies, (2) a clarification of a role of internal nonadiabaticity, which is not considered in Ref. 24.

The present work partly fills this gap, representing a straightforward continuation and further development of the strong-coupling approach described in Ref. 24. The goal of the present treatment is to derive a polaron optical conductivity that is asymptotically exact in the strong-coupling limit, at least in the leading order in powers of the inverse to the polaron coupling constant. We develop the multiphonon strong-coupling expansion using numerically accurate in the strong-coupling limit polaron energies and wave functions and accounting for the internal nonadiabaticity. In fact, the present work is a part of the project started in Ref. 11 and continued in Refs. 18 and 24 (see also references therein).

The paper is organized as follows. In Sec. II, the strong-coupling polaron optical conductivity is derived. In Sec. III, the numerical results for the polaron optical conductivity are discussed. Section IV contains conclusions.

II. OPTICAL CONDUCTIVITY

We consider the electron-phonon system with the Hamiltonian written down in the Feynman units ($\hbar = 1$, the carrier band mass $m_b = 1$, and the LO-phonon frequency $\omega_{\rm LO} = 1$):

$$H = \frac{\mathbf{p}^2}{2} + \sum_{\mathbf{q}} \left(b_{\mathbf{q}}^{+} b_{\mathbf{q}} + \frac{1}{2} \right) + \sum_{\mathbf{q}} V_{\mathbf{q}} (b_{\mathbf{q}} + b_{-\mathbf{q}}^{+}) e^{i\mathbf{q}\cdot\mathbf{r}}, \quad (1)$$

where $\mathbf{r}, \mathbf{p}$ represent the position and momentum of an electron, $b_{\mathbf{q}}^{+}, b_{\mathbf{q}}$ denote the creation and annihilation operators for longitudinal optical (LO) phonons with wave vector $\mathbf{q}$, and $V_{\mathbf{q}}$ describes the amplitude of the interaction between the electrons and the phonons. For the Fröhlich electron-phonon interaction, the amplitude of the electron–LO-phonon interaction is

$$V_{\mathbf{q}} = \frac{1}{\sqrt{V}} \frac{\sqrt{2\sqrt{2}\pi\alpha}}{q} \quad (2)$$

with the crystal volume V and the electron-phonon coupling constant α.

The polaron optical conductivity describes the response of the system with the Hamiltonian (1) to an applied electromagnetic field (along the z axis) with frequency ω. This optical response is expressed using the Kubo formula with a dipole-dipole correlation function:

$$\mathrm{Re}\,\sigma(\omega) = \frac{n_0 \omega}{2} (1 - e^{-\beta\omega}) \int_{-\infty}^{\infty} e^{i\omega t} \langle d_z(t) d_z \rangle \, dt, \quad (3)$$

where $\mathbf{d} = -e_0 \mathbf{r}$ is the electric dipole moment, e_0 is the unit charge, $\beta = \frac{1}{k_B T}$, n_0 is the electron density. In the zero-temperature limit, the optical conductivity (3) measured in units of e_0^2 becomes

$$\mathrm{Re}\,\sigma(\omega) = \frac{\omega}{2} \int_{-\infty}^{\infty} e^{i\omega t} f_{zz}(t) \, dt, \quad (4)$$

with the correlation function

$$f_{zz}(t) \equiv \langle z(t) z(0) \rangle = \langle \Psi_0 | e^{itH} z e^{-itH} z | \Psi_0 \rangle, \quad (5)$$

where $|\Psi_0\rangle$ is the ground-state wave function of the electron-phonon system.

The approach that is valid in the strong-coupling limit for the electron-phonon system is the *adiabatic approximation* (for details, see, e.g., Ref. 26) The adiabatic approximation is based on the physical reasoning that, when the electron-phonon coupling is sufficiently strong, the polaron potential well is deep and narrow, and hence the energy difference between the ground state and the first excited state can be large with respect to the LO-phonon energy. Under these conditions, the electron is a "fast" subsystem, and the phonons are a "slow" subsystem. Therefore the electron motion can adiabatically follow the phonon configuration, while the phonon motion can be considered at the background of the averaged electron motion. In this connection, the trial wave function within the adiabatic approximation is chosen as a product of an electron wave function $\psi_0(\mathbf{r}, \{Q_{\mathbf{q}}\})$ to a phonon wave function $\Phi_{\rm ph}(\{Q_{\mathbf{q}}\})$, where r is the electron coordinate vector, and $\{Q_{\mathbf{q}}\}$ are the phonon coordinates. Here, we use the complex phonon coordinates $Q_{\mathbf{q}}$ and moments $P_{\mathbf{q}}$ related to the annihilation and creation operators of the phonons by

$$Q_{\mathbf{q}} = \frac{a_{\mathbf{q}} + a_{-\mathbf{q}}^{+}}{\sqrt{2}}, \quad P_{\mathbf{q}} = i \frac{a_{\mathbf{q}}^{+} - a_{-\mathbf{q}}}{\sqrt{2}}. \quad (6)$$

The details and the substantiation of the adiabatic approximation are represented in Appendix A. Within the adiabatic approximation, the trial variational ground-state wave function is chosen as the product of a trial wave function of an electron $|\psi_0\rangle$ and of a trial wave function of a phonon subsystem $|\Phi_{\rm ph}\rangle$:

$$|\Psi_0\rangle = |\psi_0\rangle |\Phi_{\rm ph}\rangle. \quad (7)$$

The phonon trial wave function is written as the strong-coupling unitary transformation applied to the phonon vacuum:

$$|\Phi_{\rm ph}\rangle = U |0_{\rm ph}\rangle. \quad (8)$$

with the unitary operator

$$U = e^{\sum_{\mathbf{q}} (f_{\mathbf{q}} b_{\mathbf{q}} - f_{\mathbf{q}}^{*} b_{\mathbf{q}}^{+})}, \quad (9)$$

and the variational parameters $\{f_{\mathbf{q}}\}$. The transformed Hamiltonian $\tilde{H} \equiv U^{-1}HU$ takes the form

$$\tilde{H} = \tilde{H}_0 + W \tag{10}$$

with the terms

$$\tilde{H}_0 = \frac{\mathbf{p}^2}{2} + \sum_{\mathbf{q}} |f_{\mathbf{q}}|^2 + V_a(r) + \sum_{\mathbf{q}} \left(b_{\mathbf{q}}^+ b_{\mathbf{q}} + \frac{1}{2} \right), \tag{11}$$

$$W = \sum_{\mathbf{q}} (W_{\mathbf{q}} b_{\mathbf{q}} + W_{\mathbf{q}}^* b_{\mathbf{q}}^+). \tag{12}$$

Here, $W_{\mathbf{q}}$ are the amplitudes of the renormalized electron-phonon interaction

$$W_{\mathbf{q}} = \frac{\sqrt{2\sqrt{2}\pi\alpha}}{q\sqrt{V}} (e^{i\mathbf{q}\cdot\mathbf{r}} - \rho_{\mathbf{q},0}), \tag{13}$$

where $\rho_{\mathbf{q},0}$ is the expectation value of the operator $e^{i\mathbf{q}\cdot\mathbf{r}}$ with the trial electron wave function $|\psi_0\rangle$:

$$\rho_{\mathbf{q},0} = \langle \psi_0 | e^{i\mathbf{q}\cdot\mathbf{r}} | \psi_0 \rangle, \tag{14}$$

and $V_a(r)$ is the self-consistent potential energy for the electron,

$$V_a(r) = -\sum_{\mathbf{q}} \frac{4\sqrt{2}\pi\alpha}{q^2 V} \rho_{-\mathbf{q},0} e^{i\mathbf{q}\cdot\mathbf{r}}. \tag{15}$$

Averaging the Hamiltonian (10) with the phonon vacuum $|0\rangle$ and with the trial electron wave function $|\psi_0\rangle$, we arrive at the following variational expression for the ground-state energy:

$$E_0 = \langle \Psi_0 | H | \Psi_0 \rangle = \langle \psi_0 | \frac{\mathbf{p}^2}{2} | \psi_0 \rangle + \sum_{\mathbf{q}} |f_{\mathbf{q}}|^2 - \sum_{\mathbf{q}} (V_{\mathbf{q}} f_{\mathbf{q}}^* \rho_{\mathbf{q},0} + V_{\mathbf{q}}^* f_{\mathbf{q}} \rho_{-\mathbf{q},0}). \tag{16}$$

After minimization of the polaron ground-state energy (16), the parameters $f_{\mathbf{q}}$ acquire their optimal values

$$f_{\mathbf{q}} = V_{\mathbf{q}} \rho_{\mathbf{q},0}. \tag{17}$$

The ground-state energy with $\{f_{\mathbf{q}}\}$ given by Eq. (17) takes the form

$$E_0 = \langle \psi_0 | \frac{\mathbf{p}^2}{2} | \psi_0 \rangle - \sum_{\mathbf{q}} |V_{\mathbf{q}}|^2 |\rho_{\mathbf{q},0}|^2. \tag{18}$$

With the strong-coupling ansatz (7) for the polaron ground-state wave function and after the application of the unitary transformation (9), the correlation function (5) takes the form

$$f_{zz}(t) = \langle 0_{\mathrm{ph}} | \langle \psi_0 | e^{it\tilde{H}} z e^{-it\tilde{H}} z | \psi_0 \rangle | 0_{\mathrm{ph}} \rangle. \tag{19}$$

This correlation function can be expanded using a complete orthogonal set of intermediate states $|j\rangle$ and the completeness property:

$$\sum_j |j\rangle \langle j| = 1. \tag{20}$$

In the present work, we use the intermediate basis of the Franck-Condon (FC) states. The FC states correspond to the equilibrium phonon configuration for the ground state. Thus the FC wave functions are the exact eigenstates of the Hamiltonian $\tilde{H}_0$. Further on, the FC wave functions are written in the spherical-wave representation as $|\psi_{n,l,m}\rangle = R_{n,l}(r) Y_{l,m}(\theta,\varphi)$, where $R_{n,l}(r)$ are the radial wave functions, $Y_{l,m}(\theta,\varphi)$ are the spherical harmonics, l is the quantum number of the angular momentum, m is the z projection of the angular momentum, and n is the radial quantum number. In this classification, the ground-state wave function is $|\psi_{0,0,0}\rangle \equiv |\psi_0\rangle$. The energy levels for the eigenstates of the Hamiltonian $\tilde{H}_0$ are denoted $E_{n,l}$.

Using (20) with that complete and orthogonal basis, we transform (19) to the expression

$$f_{zz}(t) = \sum_{\substack{n,l,m,\\ n',l',m',\\ n'',l'',m''}} \langle \psi_{n,l,m} | z | \psi_{n'',l'',m''} \rangle \langle \psi_{n',l',m'} | z | \psi_0 \rangle \langle 0_{\mathrm{ph}} | \times \langle \psi_0 | e^{it\tilde{H}} | \psi_{n,l,m} \rangle \langle \psi_{n'',l'',m''} | e^{-it\tilde{H}} | \psi_{n',l',m'} \rangle | 0_{\mathrm{ph}} \rangle. \tag{21}$$

The correlation function (21) is transformed in the following way. The exponents $e^{it\tilde{H}}$ and $e^{-it\tilde{H}}$ are disentangled:

$$e^{-it\tilde{H}} = e^{-it\tilde{H}_0} \mathrm{T} \exp\left(-i \int_0^t ds\, W(s) \right), \tag{22}$$

$$e^{it\tilde{H}} = e^{it\tilde{H}_0} \mathrm{T} \exp\left(i \int_0^t ds\, W(-s) \right), \tag{23}$$

where $W(s)$ is the renormalized electron-phonon interaction Hamiltonian W in the interaction representation:

$$W(s) \equiv e^{is\tilde{H}_0} W e^{-is\tilde{H}_0}. \tag{24}$$

This gives us the result

$$f_{zz}(t) = \sum_{\substack{n,l,m,\\ n',l',m',\\ n'',l'',m''}} \langle \psi_{n,l,m} | z | \psi_{n'',l'',m''} \rangle \langle \psi_{n',l',m'} | z | \psi_0 \rangle e^{it(E_0 - E_{n'',l''})} \times \langle 0_{\mathrm{ph}} | \langle \psi_0 | S^+(t) | \psi_{n,l,m} \rangle \langle \psi_{n'',l'',m''} | S(t) | \psi_{n',l',m'} \rangle | 0_{\mathrm{ph}} \rangle, \tag{25}$$

with the evolution operator for the renormalized electron-phonon interaction:

$$S(t) = \mathrm{T} \exp\left(-i \int_0^t ds\, W(s) \right). \tag{26}$$

So far, the only approximation made in (21) is the strong-coupling ansatz for the polaron ground-state wave function. However, in order to obtain a numerically tractable expression for the polaron optical conductivity, an additional approximation valid in the strong-coupling limit must be applied to the matrix elements of the evolution operator $S(t)$. As discussed in Appendix A, this strong-coupling ansatz is consistent with the adiabatic approximation.[26] Within the adiabatic approximation, the vibration motion of the lattice is assumed to be slow with respect to the motion of the electron. This assumption is based on the fact that in the strong-coupling regime, the electron moves in a deep potential

well, so that the transition frequency between the ground and excited states is high with respect to the LO-phonon frequency. As far as the electron adiabatically follows the lattice vibrations, the transition probabilities due to the electron-phonon interaction[27] for the transitions between the ground and excited states are small in the strong-coupling limit with respect to those between different states of a degenerate excited energy level (or different excited states with close energies). Indeed, an effective range of integration over space in the matrix elements of the electron-phonon interaction is of the order of the width of the polaron potential well. In the strong-coupling limit, this range diminishes approximately as α^{-1}. Correspondingly, the exponent $e^{i\mathbf{q}\cdot\mathbf{r}}$ within this spatial extent in the strong-coupling limit is close to unity, and hence the matrix elements of the aforesaid exponent tend to the orthogonality integrals, which are zero when the initial and final states are different. Moreover, the transition probabilities between the ground and excited states fall down at strong coupling due to an increasing energy difference between these states. Therefore we neglect the matrix elements of the evolution operator (26) between the ground and excited states. Physically, this approximation is consistent with the Franck-Condon principle: an electronic transition is most likely to occur at a "frozen" motion of a phonon subsystem. The Franck-Condon principle (just in the same scheme as in the present work) is frequently used in the theory of multi-phonon atomic and impurity optical spectra (see, e.g., Refs. 15 and 28). It should be noted that the Franck-Condon principle and the strong-coupling ansatz are not additional approximations with respect to the adiabatic approximation: they straightforwardly follow from the adiabatic approach.

Effects beyond the adiabatic approximation for the transition due to the electron-phonon interaction between the ground and excited states (neglected here) are often called "the external nonadiabaticity." On the contrary, the "internal nonadiabaticity" related to the transitions between different excited states is taken into account in the present work. In other words, the nondiagonal matrix elements of the evolution operator between different excited states are accounted for. The internal nonadiabaticity results in the static and dynamic Jahn-Teller effect.

Strictly speaking, the summation over the excited polaron states in Eq. (21) must involve the transitions to both the discrete and continuous parts of the polaron spectrum. A transition to the states of the continuous spectrum means that the electron leaves the polaron potential well. Therefore these transitions can be attributed to the "polaron dissociation." The transitions to the continuous spectrum are definitely beyond the adiabatic approximation. As shown in Ref. 15, the transition probability to the states of the continuous spectrum is very small compared with the transition probability between the ground and the first excited state (which belongs to the discrete part of the polaron energy spectrum). We neglect here the contribution to the polaron optical conductivity due to the transitions to the continuous spectrum.

The matrix elements neglected within the adiabatic approximation correspond to the transitions between FC states with different energies due to the electron-phonon interaction. Hence these transitions can be called nonadiabatic. The adiabatic approximation is related to the matrix elements of the evolution operator $S(t)$. On the contrary, the matrix elements of the transitions between different FC states for the electric dipole moment are, in general, not equal to zero. Moreover, these transitions can be accompanied by the emission of phonons. The electron FC wave functions constitute a complete orthogonal set. However, the corresponding phonon wave functions can be nonorthogonal because of a different shift of phonon coordinates for different electron states. This makes multiphonon transitions possible.[28] It is important to note that in our treatment we neglect only the nonadiabatic transitions between the electron states with *different* energies. On the contrary, the transitions within one and the same degenerate level can be nonadiabatic. This *internal nonadiabaticity* (i.e., the nonadiabaticity of the transitions within one and the same degenerate level) is taken into account in the subsequent treatment.

The full details of the further derivation are described in the Appendix B. First, within the adiabatic approximation and using the selection rules for the dipole matrix elements, the correlation function (25) is reduced to the form

$$f_{zz}(t) = \sum_n D_n e^{-i\Omega_{n,0}t} \langle\psi_{n,1,0}|\langle 0_{\rm ph}| \times \mathrm{T}\exp\left[-i\int_0^t ds\, W(s)\right]|0_{\rm ph}\rangle|\psi_{n,1,0}\rangle, \quad (27)$$

where $\Omega_{n,0}$ is the FC transition frequency

$$\Omega_{n,0} \equiv E_{n,1} - E_0, \quad (28)$$

and D_n is the squared modulus of the dipole transition matrix element,

$$D_n = |\langle\psi_0|z|\psi_{n,1,0}\rangle|^2. \quad (29)$$

Second, the averaging of the operator T exponent in (27) with the electron wave functions can be exactly performed. As a result, the optical conductivity is transformed to the expression

$$\mathrm{Re}\,\sigma(\omega) = \frac{\omega}{6}\sum_n D_n \int_{-\infty}^{\infty} e^{i(\omega-\Omega_{n,0})t}\langle 0_{\rm ph}| \times \mathrm{Tr}\left(\mathrm{T}\exp\left[-i\int_0^t ds\, \mathbb{W}^{(n)}(s)\right]\right)|0_{\rm ph}\rangle dt. \quad (30)$$

The T exponent in (30) contains the finite-dimensional matrix $\mathbb{W}^{(n)}(s)$ depending on the phonon coordinates:

$$\left(\mathbb{W}^{(n)}_{k,l,m}\right)_{m_1,m_2} = \left\langle\psi_{n,1,m_1}\middle|W_{k,l,m}\middle|\psi_{n,1,m_2}\right\rangle, \quad (31)$$

where $W_{k,l,m}$ are the amplitudes of the electron-phonon interaction in the basis of spherical wave functions.

Because the kinetic energy of the phonons is of order α^{-4} compared to the leading term of the Hamiltonian,[26] we neglect this kinetic energy in the present work, because the treatment is related to the strong-coupling regime. As a result, $Q_{k,l,m}$ commute with the Hamiltonian $\tilde{H}_0$, so that in (30), $\mathbb{W}^{(n)}(s) = \mathbb{W}^{(n)}$. Furthermore, in a finite-dimensional basis $\{|\psi_{n,l,m}\rangle\}$ for a given level (n,l), all eigenvalues of the Hamiltonian $\tilde{H}_0$ are the same. Therefore the T exponent entering (30) in that finite-dimensional basis turns into a usual exponent. As a result, the strong-coupling polaron optical conductivity (30) takes the

form

$$\mathrm{Re}\,\sigma(\omega) = \frac{\omega}{6}\sum_n D_n \int_{-\infty}^{\infty} e^{i(\omega-\Omega_{n,0})t}\langle 0_{\mathrm{ph}}| \times \mathrm{Tr}\exp(-i\,\mathbb{W}^{(n)}t)|0_{\mathrm{ph}}\rangle dt. \quad (32)$$

The matrix interaction Hamiltonian (31) depends on the phonon coordinates, and the matrices $\mathbb{W}^{(n)}_{k,l,m}$ with different m for one and the same degenerate energy level do not commute with each other. According to the Jahn-Teller theorem,[29] for a degenerate level there does not exist a unitary transformation that simultaneously diagonalizes all matrices $\mathbb{W}^{(n)}_{k,l,m}$ in a basis that does not depend on the phonon coordinates. The manifestations of that theorem are attributed to the dynamic Jahn-Teller effect. Therefore, because we neglect the noncommutation of the matrices $\mathbb{W}^{(n)}_{k,l,m}$, the dynamic Jahn-Teller effect is omitted. However, the static Jahn-Teller effect is captured by formula (32), because both diagonal and nondiagonal matrix elements of the matrices $\mathbb{W}^{(n)}_{k,l,m}$ are involved in the summation.

Also the dynamic Jahn-Teller effect can be taken into account. The averaging in Eq. (32) is performed exactly using the effective phonon modes similarly to Ref. 30 (see the details in Appendix C). As a result, we arrive at the following expression for the strong-coupling polaron optical conductivity:

$$\mathrm{Re}\,\sigma(\omega) = \frac{\omega}{3\pi^2}\sum_n \frac{D_n}{a_0^{(n)}}\int_{-\infty}^{\infty}dx_0\int_{-\infty}^{\infty}dx_1\int_{-\infty}^{\infty}dx_2\int_{-\infty}^{\infty}dy_1\int_{-\infty}^{\infty}dy_2 \times \sum_{j=1}^{3}\exp\left\{-\frac{1}{2}\left[x_0^2+\sum_{m=1,2}\left(x_m^2+y_m^2\right)+\frac{\left(\omega-\Omega_{n,0}-\frac{a_2^{(n)}}{2\sqrt{5\pi}}\lambda_j(Q_2)\right)^2}{\left(a_0^{(n)}\right)^2}\right]\right\}. \quad (33)$$

Here, $\lambda_j(Q_2)$ are the eigenvalues for the matrix interaction Hamiltonian, which are explicitly determined in the Appendix C by the formula (C20). The coefficients $a_0^{(n)}$ and $a_2^{(n)}$ are given by (C11) and (C12), respectively. The polaron optical conductivity, given by the expression (33), is, in fact, an envelope of the multiphonon polaron optical conductivity band with the correlation function (30) provided by the phonon assisted transitions from the polaron ground state to the polaron RES. This result is consistent with Ref. 11, where the same paradigm of the phonon assisted transitions to the polaron RES was exploited, but the calculation was limited to the one-phonon transition.

In order to reveal the significance of the dynamic Jahn-Teller effect for the polaron, we alternatively calculate $\langle 0_{\mathrm{ph}}|\mathrm{Tr}\exp(-i\,\mathbb{W}^{(n)}t)|0_{\mathrm{ph}}\rangle$ neglecting the noncommutation of the matrices $\mathbb{W}^{(n)}_{k,l,m}$, as described in Appendix C 2. The resulting expression for the polaron optical conductivity is much simpler than formula (33) and is similar to the expression (3) of Ref. 24:

$$\mathrm{Re}\,\sigma(\omega) = \omega\sum_n \sqrt{\frac{\pi}{2\omega_s^{(n)}}}D_n\exp\left(-\frac{(\omega-\Omega_{n,0})^2}{2\omega_s^{(n)}}\right), \quad (34)$$

with the parameter (often called the Huang-Rhys factor)

$$\omega_s^{(n)} = \frac{1}{2}\left(a_0^{(n)}\right)^2 + \frac{1}{4\pi}\left(a_2^{(n)}\right)^2. \quad (35)$$

The strong-coupling electron energies and wave functions in Eq. (30) can be calculated using different approximations. For example, within the Landau-Pekar (LP) approximation,[25] the trial wave function $|\psi_0\rangle$ is chosen as the ground state of a 3D oscillator. Within the Pekar approximation,[15] $|\psi_0\rangle$ is chosen in the form

$$|\psi_0(r)\rangle = Ce^{-ar}(1+ar+br^2) \quad (36)$$

with the variational parameters a and b. Finally, the trial ground-state wave function can be determined numerically exactly following Miyake[31] (see also Ref. 32, Chap. 5.22). Within the LP approximation, formula (34) reproduces the polaron optical conductivity obtained in Ref. 24.

If we use the electron trial wave functions $|\psi_{n,l,m}\rangle$, e.g., within the Landau-Pekar approach, they are oscillatorlike, and hence all matrix elements $\langle\psi_0|z|\psi_{n,1,0}\rangle$ except that with $n=1$ (i.e., for the $1s\to 2p$ transition) are exactly equal to zero. Beyond the LP approximation, also the transitions to other excited states are allowed because of the nonparabolicity of the self-consistent potential $V_a(r)$. The use of exact strong-coupling wave functions, instead of the LP wave functions, can influence the optical conductivity. In the present treatment, we use the numerically exact electron energies and wave functions of both ground and first excited states according to Ref. 31. However, with other trial wave functions (even within the numerically exact in the strong-coupling limit Miyake's approach), the matrix element $\langle\psi_0|z|\psi_{1,1,0}\rangle$ between the ground and first excited states brings a dominating contribution to the optical conductivity, because the self-consistent potential within the extent of these two states is only slightly nonparabolic. This conclusion is confirmed also by the calculation of the relative contribution of the transitions to the upper polaron states to the zeroth frequency moment of the optical conductivity discussed below. Moreover, as far as the physics of the F centers is close to the physics of polarons, the above conclusion is also in line with the results by Pekar,[15] who showed that the relative contribution to the optical absorption of the F centers due to the transitions to the continuous part of the electron states is small with respect to the contribution of the transitions to the first excited state. Consequently, for the numerical calculations we restrict the summation in (B21) by the term with $n=1$. The FC transition energies $\Omega_{n,0}$ to leading order of the strong-coupling approximation are determined according to (28). In order to account for the corrections of the FC energy with accuracy up to α^0, we add to $\Omega_{n,0}$ the correction $\Delta\Omega_{\mathrm{FC}}\approx -3.8$ from Ref. 24.

III. RESULTS AND DISCUSSION

In Figs. 2 and 3, we have plotted the polaron optical conductivity spectra calculated for different values of the coupling constant α. The optical conductivity spectra calculated within the present strong-coupling approach taking into account the Jahn-Teller effect are shown by the solid curves. The optical conductivity derived neglecting the Jahn-Teller effect is shown by the dashed curves. It is worth mentioning that there is little difference in the optical conductivity spectra between those calculated with and without the Jahn-Teller effect. The optical conductivity obtained in Ref. 24 with the Landau-Pekar (LP) adiabatic approximation is plotted with dash-dotted curves. The full dots show the numerical diagrammatic quantum Monte Carlo (DQMC) data.[21,24] The FC transition frequency for the transition to the first excited FC state $\Omega_{1,0} \equiv \Omega_{FC}$ and the RES transition frequency Ω_{RES} are explicitly indicated in the figures.

The polaron optical conductivity spectra calculated within the present strong-coupling approach are shifted to lower frequencies with respect to the optical conductivity spectra calculated within the LP approximation of Ref. 24. This shift is due to the use of the numerically accurate strong-coupling energy levels and wave functions of the internal polaron states and of the numerically accurate self-consistent adiabatic polaron potential.

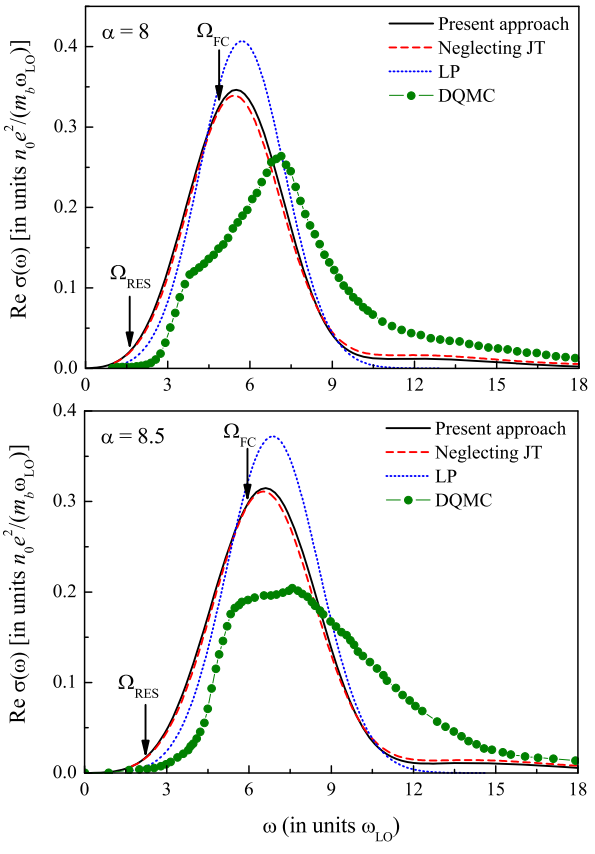

FIG. 2. (Color online) Strong-coupling polaron optical conductivity calculated within the strong-coupling approach of the present work accounting for the dynamic Jahn-Teller effect (solid curves), accounting for the static Jahn-Teller effect (dashed curves), within the adiabatic approximation of Ref. 24 (dot-dashed curves), and the numerical diagrammatic Monte Carlo data (full dots) for $\alpha = 8$ and 8.5. The FC and RES transition frequencies are indicated by the arrows.

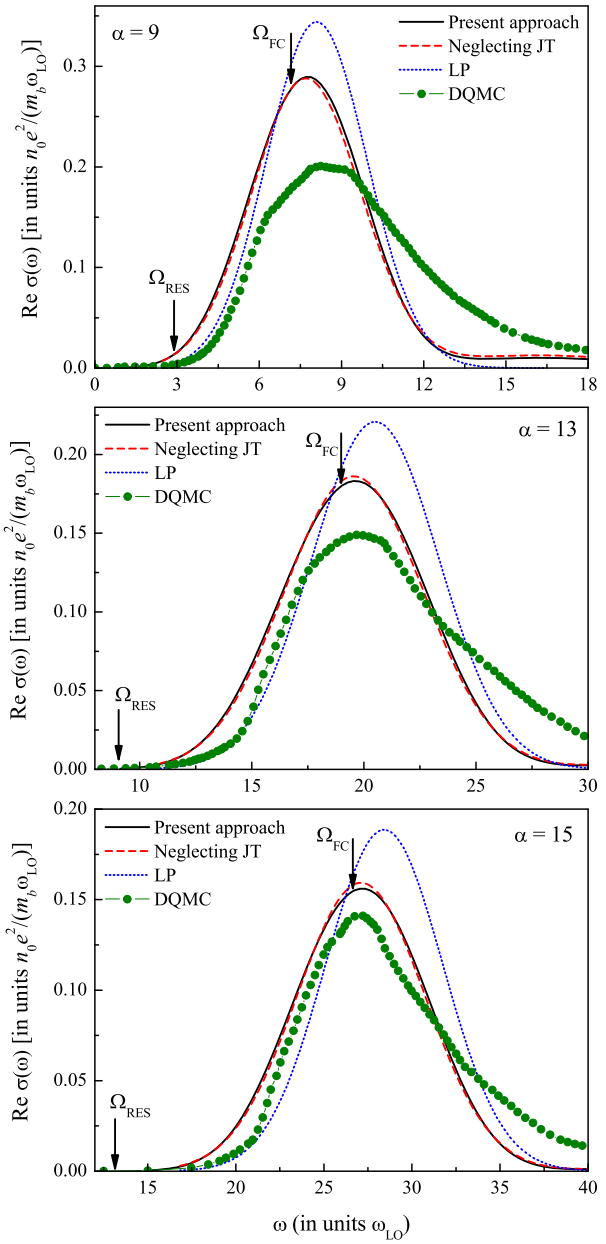

FIG. 3. (Color online) The same as in Fig. 2 for $\alpha = 9$, 13, and 15.

According to the selection rules for the matrix elements of the electron-phonon interaction, there is a contribution to the polaron optical conductivity from the phonon modes with angular momentum $l = 0$ (s phonons) and with angular momentum $l = 2$ (d phonons). The s phonons are fully symmetric, therefore they do not contribute to the Jahn-Teller effect, while the d phonons are active in the Jahn-Teller effect. The major contribution to the strong-coupling polaron optical conductivity is due to the electron-phonon interaction with the fully symmetric s phonons. The interaction with the s phonons strongly suppresses the manifestations of the dynamic Jahn-Teller effect. This explains a relatively small

distinction between the optical conductivity spectra calculated accounting for the static and dynamic Jahn-Teller effect. We therefore can conclude that the simplified calculation of the optical conductivity using formula (34) accounting for the static Jahn-Teller effect provides accurate results in the strong-coupling limit.

For $\alpha = 8$ and 8.5, the maxima of the polaron optical conductivity spectra, calculated within the present strong-coupling approach are positioned to the low-frequency side of the maxima of those calculated using the DQMC method. The agreement between our strong-coupling polaron optical conductivity spectra and the numerical DQMC data improves with increasing alpha. This is in accordance with the fact that the present strong-coupling approach for the polaron optical conductivity is asymptotically exact in the strong-coupling limit.

It is interesting to compare the optical conductivity of the Fröhlich polaron within the strong-coupling approximation with the optical conductivity of a Holstein polaron in 3D, calculated in Refs. 22 and 23 by two methods: the numerical DQMC and the momentum average approximation for the two-particle Green's functions. Remarkably, in the strong-coupling regime, the analytically determined large-polaron and small-polaron optical conductivity spectra exhibit similar shapes. This result is not surprising, because the large-polaron and small-polaron models in fact describe one and the same physical object, but in different regimes. At a rather weak coupling, the large-polaron picture is physically more realistic, while in the strong-coupling limit, when a polaron radius becomes comparable with a lattice constant, the small polaron model can be adequate. Also for small coupling strengths, the small-polaron optical conductivity obtained in Ref. 22 strongly resembles the large-polaron optical conductivity at weak coupling from Ref. 9, except the artifact onset for the small-polaron optical conductivity which starts at $\omega < \omega_{\mathrm{LO}}$. In the intermediate coupling strength range, however, the small-polaron and large-polaron response spectra are different from each other.

The total polaron optical conductivity must satisfy the sum rule[33]

$$\int_0^\infty \mathrm{Re}\,\sigma\,(\omega)\,d\omega = \frac{\pi}{2}. \tag{37}$$

In the weak- and intermediate-coupling regimes at $T = 0$, there are two contributions to the left-hand side of that sum rule: (1) the contribution from the polaron optical conductivity for $\omega > \omega_{\mathrm{LO}}$ and (2) the contribution from the "central peak" at $\omega = 0$, which is proportional to the inverse polaron mass.[33] In the asymptotic strong-coupling regime, the inverse to the polaron mass is of order α^{-4}, and hence the contribution from the "central peak" to the polaron optical conductivity is beyond the accuracy of the present approximation (where we keep the terms $\propto\alpha^{-2}$ and $\propto\alpha^{0}$).

As discussed above, in the present work, the transitions from the ground state to the states of the continuous part of the polaron energy spectrum are neglected. Therefore the integral over the frequency [the left-hand side of (37)] for the optical conductivity calculated within the present strong-coupling approximation can be (relatively slightly) smaller than $\pi/2$. The relative contribution of the transitions to the continuous part of the polaron spectrum, Δ_c, can be therefore estimated as

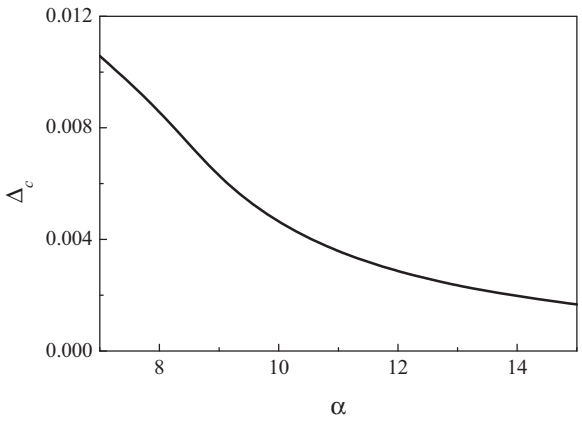

FIG. 4. Relative contribution of the transitions to the continuum polaron states to the zeroth frequency moment of the strong-coupling polaron optical conductivity as a function of the coupling constant α.

$$\Delta_c \equiv 1 - \frac{2}{\pi}\int_0^\infty \mathrm{Re}\,\sigma\,(\omega)\,d\omega, \tag{38}$$

where the right-hand side is obtained by a numerical integration of $\mathrm{Re}\,\sigma\,(\omega)$ calculated within the present strong-coupling approach. This numeric estimation shows that for $\alpha > 8$, $\Delta_c < 0.01$. Moreover, with increasing α, the relative contribution of the transitions to the continuous part of the polaron spectrum falls down. This confirms the accuracy of the present strong-coupling approach.

In Refs. 13 and 14, the optical conductivity of a strong-coupling polaron was calculated assuming that in the strong-coupling regime the polaron optical response is provided mainly by the transitions to the continuous part of the spectrum (these transitions are called there "the polaron dissociation"). This concept is in contradiction both with the early estimation by Pekar[15] discussed above and with the very small weight of those transitions shown in Fig. 4. The approach of Ref. 13 in fact takes into account only a small part of the strong-coupling polaron optical conductivity–namely, the high-frequency "tail" of the optical conductivity spectrum.

When comparing the polaron optical conductivity spectra calculated in the present work with the DQMC data,[21,24] we can see that the present approach, with respect to DQMC, underestimates the high-frequency part of the polaron optical conductivity. This difference remains not very small even for relatively large $\alpha = 15$. We do not yet possess DQMC results for the polaron optical conductivity at higher coupling strengths for a comparison of the present calculation with them. However, it is worth noting that the aforesaid difference, especially concerning the position of the maximum of the optical conductivity spectrum, gradually decreases with increasing α. We can also note on an improvement of accuracy with respect to Ref. 24 due to use of more accurate trial polaron states with respect to the LP approach.

Because the optical conductivity spectra calculated in the present strong-coupling approximation using the expressions (33) and (34) represent the envelopes of the RES peak with the multiphonon satellites, the separate peeks are not explicitly

seen in those spectra. The FC and RES peaks are indicated in the figures by the arrows. The FC transition frequency $\Omega_{1,0}$ in the strong-coupling case is positioned close to the maximum of the polaron optical conductivity band (both calculated within the present approach and within DQMC). The RES transition frequency is positioned one ω_{LO} below the onset of the LO sidebands. Note that the strong-coupling polaron optical conductivity derived in Ref. 34 contains only the zero-phonon (RES) line and no phonon satellites at all. In contrast, in the present calculation, the maximum of the polaron optical conductivity spectrum shifts to higher frequencies with increasing α, so that the multiphonon processes invoking large number of phonons become more and more important, in accordance with predictions of Refs. 11 and 18.

It is worth noting the following important point: the maximum of the polaron optical conductivity band can be hardly interpreted as a broadened transition to an FC state on the following reasons. Formula (30) describes a set of multiphonon peaks. In the simplifying approximation which neglects the Jahn-Teller effect (see Ref. 24), those peaks are positioned at the frequencies $\omega = \tilde{\Omega}_{n,0} + k$, where k is the number of emitted phonons and $\tilde{\Omega}_{n,0}$ is the frequency of the zero-phonon line. The frequencies $\tilde{\Omega}_{n,0}$ do not coincide with the FC transition frequencies but are determined by

$$\tilde{\Omega}_{n,0} = \Omega_{n,0} - \omega_s^{(n)}, \tag{39}$$

where the Huang-Rhys factor $\omega_s^{(n)}$ describes the energy shift due to lattice relaxation. The physical meaning of the parameters $\omega_s^{(n)}$ obviously implies that the peaks at $\omega = \tilde{\Omega}_{n,0} + k$ should be attributed to transitions to the RES with emission of k phonons. So, the so-called "FC transition" is realized as the envelope of a series of phonon sidebands of the polaron RES but not as a transition to the FC state. The account of the Jahn-Teller effects in general makes the multiphonon peak series nonequidistant, but it changes nothing in the concept of the internal polaron states that is discussed above.

IV. CONCLUSIONS

We have derived the polaron optical conductivity, which is asymptotically exact in the strong-coupling limit. The strong-coupling polaron optical conductivity band is provided by the multiphonon transitions from the polaron ground state to the polaron RES and has the maximum positioned close to the FC transition frequency. With increasing the electron-phonon coupling constant α, the polaron optical conductivity band shape gradually tends to that provided by the diagrammatic quantum Monte Carlo (DQMC) method. This agreement demonstrates the importance of the multiphonon processes for the polaron optical conductivity in the strong-coupling regime.

The obtained polaron optical conductivity with a high accuracy satisfies the sum rule,[33] which gives us an evidence of the fact that in the strong-coupling regime the dominating contribution to the polaron optical conductivity is due to the transitions to the internal polaron states, while the contribution due to the transitions to the continuum states is negligibly small.

Accurate numerical results, obtained using DQMC method,[21]—modulo the linewidths for sufficiently large α—and the analytically exact in the strong-coupling limit polaron optical conductivity of the present work, as well as the analytical approximation of Ref. 24, confirm the essence of the mechanism for the optical absorption of Fröhlich polarons, which were proposed in Refs. 18 and 19.

ACKNOWLEDGMENTS

One of the authors (J.T.D.) thanks R. Evrard and E. Kartheuser for early collaboration that led to Ref. 11 that contains key- conceptual elements for the present work. J.T.D. also thanks A. S. Mishchenko for providing his (unpublished) DQMC results for large coupling and for stimulating discussions related to his DQMC. We thank F. Brosens, H. Kleinert, G. Iadonisi, V. M. Fomin, G. De Filippis, and V. Cataudella for valuable discussions. This work was supported by FWO-V projects G.0356.06, G.0370.09N, G.0180.09N, G.0365.08, the WOG WO.035.04N (Belgium).

APPENDIX A: ADIABATIC APPROXIMATION FOR POLARONS

In order to substantiate the strong-coupling scheme briefly represented in Sec. II, we describe here the rigorous derivation of the adiabatic approximation following Refs. 15 and 26 in terms of the complex phonon coordinates, which are preferable with respect to real coordinates used in Refs. 15 and 26 for the calculation of the optical response. The Hamiltonian of the electron-phonon system (1) is equivalently expressed in terms of the complex phonon coordinates as follows:

$$H = \frac{\mathbf{p}^2}{2} + \frac{1}{2}\sum_{\mathbf{q}} \left(P_{\mathbf{q}} P_{-\mathbf{q}} + \omega_{\mathbf{q}}^2 Q_{\mathbf{q}} Q_{-\mathbf{q}} - 1\right) + \sqrt{2}\sum_{\mathbf{q}} V_{\mathbf{q}} Q_{\mathbf{q}} e^{i\mathbf{q}\cdot\mathbf{r}}, \tag{A1}$$

where $P_{\mathbf{q}}$ and $Q_{\mathbf{q}}$ are the operators of complex phonon moments and coordinates, respectively. Here, we assume, for generality, dispersive optical phonons with the frequencies $\omega_{\mathbf{q}}$.

The exact Schrödinger equation for the total electron-phonon wave function is

$$H\Psi_s(\mathbf{r}, Q) = E_s \Psi_s(\mathbf{r}, Q)\ (Q \equiv \{Q_{\mathbf{q}}\}), \tag{A2}$$

where the index s labels the eigenfunctions $\Psi_s(\mathbf{r}, Q)$ and the eigenvalues E_s of the Hamiltonian H.

Let us denote H_e the electron part of the Hamiltonian

$$H_e \equiv \frac{\mathbf{p}^2}{2} + \sqrt{2}\sum_{\mathbf{q}} V_{\mathbf{q}} Q_{\mathbf{q}} e^{i\mathbf{q}\cdot\mathbf{r}}. \tag{A3}$$

The approach for the Schrödinger equation (A2) appropriate in the strong-coupling regime is the adiabatic approximation.[15,26] Within the adiabatic approximation, the electron moving in its potential well (induced by lattice polarization) is assumed to be a "fast" subsystem, while the lattice vibrations are a "slow" subsystem. The physical grounds for this assumption follow from the fact that at strong electron-phonon coupling, the aforesaid potential well is sufficiently deep, so that the energy levels of the excited states are separated from the ground-state level by a large (with respect to the LO-phonon energies) energy gap.

Therefore the ground-state wave function $\Psi_0(\mathbf{r},Q)$ is chosen as the product of the electron wave function $\psi_0(\mathbf{r},Q)$, which depends on the phonon coordinates as parameters, and the phonon wave function $\Phi_{\rm ph}(Q)$, which does not depend on the electron coordinates:

$$\Psi_0(\mathbf{r},Q) = \psi_0(\mathbf{r},Q)\,\Phi_{\rm ph}(Q), \tag{A4}$$

where $\psi_0(\mathbf{r},Q)$ obeys the Schrödinger equation for the "fast" subsystem

$$H_e\psi_0(\mathbf{r},Q) = \varepsilon_0(Q)\,\psi_0(\mathbf{r},Q). \tag{A5}$$

Since the Hamiltonian H_e does not contain the moments of phonons $P_{\mathbf{q}}$, both $\varepsilon_0(Q)$ and $\psi_0(\mathbf{r},Q)$ depend on the phonon coordinates $Q_{\mathbf{q}}$ as on parameters.

The adiabatic approximation is based on the assumption that because the phonon subsystem is "slow," the electron wave function $\psi_0(\mathbf{r},Q)$ slowly varies when varying the phonon coordinates Q. Thus mathematically the adiabatic approximation is performed by neglecting the effect of the operator of the phonon kinetic energy on the electron wave function (the "nonadiabaticity operator,"Ref. 26):

$$\left[\frac{1}{2}\sum_{\mathbf{q}}(P_{\mathbf{q}}P_{-\mathbf{q}}-1)\right]\psi_0(\mathbf{r},Q)\Phi_{\rm ph}(Q) \approx \psi_0(\mathbf{r},Q)\left[\frac{1}{2}\sum_{\mathbf{q}}(P_{\mathbf{q}}P_{-\mathbf{q}}-1)\right]\Phi_{\rm ph}(Q). \tag{A6}$$

Therefore we find that

$$H\Psi_0(\mathbf{r},Q) \approx \psi_0(\mathbf{r},Q)\left[\frac{1}{2}\sum_{\mathbf{q}}\left(P_{\mathbf{q}}P_{-\mathbf{q}}+\omega_{\mathbf{q}}^2Q_{\mathbf{q}}Q_{-\mathbf{q}}\right)+\varepsilon_0(Q)\right]\times\Phi_{\rm ph}(Q). \tag{A7}$$

As a result, we arrive at the Schrödinger equation for the "slow" subsystem within the adiabatic approximation,

$$\tilde{H}_0\Phi_{\rm ph}(Q) = E_0\Phi_{\rm ph}(Q), \tag{A8}$$

where the Hamiltonian of the adiabatic approximation for the "slow" subsystem (phonons) is

$$\tilde{H}_0 \equiv \frac{1}{2}\sum_{\mathbf{q}}\left(P_{\mathbf{q}}P_{-\mathbf{q}}+\omega_{\mathbf{q}}^2Q_{\mathbf{q}}Q_{-\mathbf{q}}\right)+\varepsilon_0(Q). \tag{A9}$$

Note that the eigenvalue for the Hamiltonian (A8) of the "slow" subsystem is the total ground-state energy of the electron-phonon system.

Consistently with the adiabatic approximation, we assume that the electron wave function $\psi_0(\mathbf{r},Q)$ slowly depends on phonon coordinates Q. Therefore the Schrödinger equation for the electron subsystem can be solved using the perturbation method, where the zeroth-order approximation corresponds to the equilibrium phonon configuration Q_0. This configuration will be determined from the minimum of the total ground-state energy of the electron-phonon system. The perturbation corrections to the electron energies due to variation of phonon coordinates are considered in the first order with respect to $(Q-Q_0)$.

The Hamiltonian H_e is thus a sum of two terms:

$$H_e = H_e^{(0)} + W, \tag{A10}$$

where $H_e^{(0)}$ is the leading-order Hamiltonian of the adiabatic approximation,

$$H_e^{(0)} \equiv \frac{\mathbf{p}^2}{2} + V_a(\mathbf{r}), \tag{A11}$$

with the potential

$$V_a(\mathbf{r}) = \sqrt{2}\sum_{\mathbf{q}}V_{\mathbf{q}}Q_{\mathbf{q},0}e^{i\mathbf{q}\cdot\mathbf{r}}, \tag{A12}$$

and W is the renormalized Hamiltonian of the electron-phonon interaction:

$$W = \sqrt{2}\sum_{\mathbf{q}}V_{\mathbf{q}}(Q_{\mathbf{q}}-Q_{\mathbf{q},0})e^{i\mathbf{q}\cdot\mathbf{r}}. \tag{A13}$$

Within the aforesaid scheme, $H_e^{(0)}$ is the zeroth-order Hamiltonian, and W is a perturbation.

Comparing the Hamiltonians (A3) and (A11), one can see that the zeroth-order approximation for the electron wave function is obtained by the replacement of the phonon coordinates in the argument of $\psi_0(\mathbf{r},Q)$ by their equilibrium values Q_0:

$$\psi_0(\mathbf{r},Q) \to \psi_0(\mathbf{r},Q_0) \equiv |\psi_0\rangle. \tag{A14}$$

The energy $\varepsilon_0(Q)$ is found within the first-order perturbation theory, where $\varepsilon_0^{(0)} \equiv \varepsilon_0(Q_0)$ is the zeroth-order approximation. The first-order perturbation correction to the electron energy is

$$\varepsilon_0^{(1)}(Q) = \langle\psi_0|W|\psi_0\rangle = \sum_{\mathbf{q}}\sqrt{2}V_{\mathbf{q}}(Q_{\mathbf{q}}-Q_{\mathbf{q},0})\rho_{\mathbf{q},0}, \tag{A15}$$

where $\rho_{\mathbf{q},0}$ is the average:

$$\rho_{\mathbf{q},0} \equiv \langle\psi_0|e^{i\mathbf{q}\cdot\mathbf{r}}|\psi_0\rangle. \tag{A16}$$

The resulting electron energy is given by

$$\varepsilon_0(Q) = \varepsilon_0(Q_0) + \sum_{\mathbf{q}}\sqrt{2}V_{\mathbf{q}}(Q_{\mathbf{q}}-Q_{\mathbf{q},0})\rho_{\mathbf{q},0}. \tag{A17}$$

As a result, the adiabatic Hamiltonian (A9) takes the form

$$\tilde{H}_0 = \frac{1}{2}\sum_{\mathbf{q}}\left(P_{\mathbf{q}}P_{-\mathbf{q}}+\omega_{\mathbf{q}}^2Q_{\mathbf{q}}Q_{-\mathbf{q}}\right)+\varepsilon_0(Q_0) + \sum_{\mathbf{q}}\sqrt{2}V_{\mathbf{q}}(Q_{\mathbf{q}}-Q_{\mathbf{q},0})\rho_{\mathbf{q},0}. \tag{A18}$$

Let us determine $Q_{\mathbf{q},0}$ as equilibrium positions for phonon coordinates. This corresponds to the following physical reasoning: we expand $\varepsilon_0(Q)$ near the point $Q = Q_0$, where $\varepsilon_0(Q)$ depends on Q most slowly. Hence the point $Q = Q_0$ corresponds to a minimum of $\varepsilon_0(Q)$. After the transformation to new (shifted) phonon coordinates $\tilde{Q}_{\mathbf{q}}$,

$$\tilde{Q}_{\mathbf{q}} \equiv Q_{\mathbf{q}} - Q_{\mathbf{q},0}, \tag{A19}$$

the Hamiltonian $\tilde{H}_0$ does not contain the terms linear with respect to $\tilde{Q}_{\mathbf{q}}$:

$$\tilde{H}_0 = \varepsilon_0(Q_0) + \frac{1}{2}\sum_{\mathbf{q}}\left(P_{\mathbf{q}}P_{-\mathbf{q}} + \omega_{\mathbf{q}}^2\tilde{Q}_{\mathbf{q}}\tilde{Q}_{-\mathbf{q}} + \omega_{\mathbf{q}}^2|Q_{\mathbf{q},0}|^2\right), \tag{A20}$$

what provides the equation for $Q_{\mathbf{q},0}$:

$$\omega_{\mathbf{q}}^2 Q_{-\mathbf{q},0} + \sqrt{2}V_{\mathbf{q}}\rho_{\mathbf{q},0} = 0. \tag{A21}$$

Therefore the equilibrium positions are

$$Q_{\mathbf{q},0} = -\frac{\sqrt{2}V_{-\mathbf{q}}\rho_{-\mathbf{q},0}}{\omega_{\mathbf{q}}^2}. \tag{A22}$$

In the new variables, the phonon Hamiltonian is the quadratic form

$$\tilde{H}_0 = J_0 + \frac{1}{2}\sum_{\mathbf{q}}\left(P_{\mathbf{q}}P_{-\mathbf{q}} + \omega_{\mathbf{q}}^2\tilde{Q}_{\mathbf{q}}\tilde{Q}_{-\mathbf{q}}\right),$$

where J_0 is the "adiabatic potential" (using the terminology of Ref. 15),

$$J_0 = \langle\psi_0|\frac{\mathbf{p}^2}{2}|\psi_0\rangle - \frac{1}{2}\Delta_0, \tag{A23}$$

with the parameter

$$\Delta_0 = \sum_{\mathbf{q}}\omega_{\mathbf{q}}^2|Q_{\mathbf{q},0}|^2 = 2\sum_{\mathbf{q}}\frac{|V_{\mathbf{q}}|^2}{\omega_{\mathbf{q}}^2}|\rho_{\mathbf{q},0}|^2. \tag{A24}$$

Let us write also the useful relation for the eigenenergy of the electron in the self-consistent potential $V_a(\mathbf{r})$:

$$\begin{aligned}\varepsilon_0^{(0)} &= J_0 - \frac{1}{2}\sum_{\mathbf{q}}\omega_{\mathbf{q}}^2|Q_{\mathbf{q},0}|^2 \\ &= \langle\psi_0|\frac{\mathbf{p}^2}{2m}|\psi_0\rangle - \sum_{\mathbf{q}}\omega_{\mathbf{q}}^2|Q_{\mathbf{q},0}|^2.\end{aligned} \tag{A25}$$

Note that the variational functional for the polaron ground-state energy is J_0 rather than $\varepsilon_0^{(0)}$.

The Schrödinger equation for the phonon subsystem takes the form

$$\begin{aligned}&\left[\frac{1}{2}\sum_{\mathbf{q}}\left(P_{\mathbf{q}}P_{-\mathbf{q}} + \omega_{\mathbf{q}}^2\tilde{Q}_{\mathbf{q}}\tilde{Q}_{-\mathbf{q}}\right)\right]\Phi_{\rm ph}(Q) \\ &\quad = (E_0 - J_0)\Phi_{\rm ph}(Q).\end{aligned} \tag{A26}$$

Now, we find the eigenenergies for the electron-phonon system within the adiabatic approximation:

$$E_0 \equiv E_0(\ldots n_{\mathbf{q}}\ldots) = J_0 + \sum_{\mathbf{q}}\hbar\omega_{\mathbf{q}}\left(n_{\mathbf{q}} + \frac{1}{2}\right), \tag{A27}$$

where the non-negative integers $\{n_{\mathbf{q}}\}$ are the numbers of real phonons. Subtracting the background of the zero-temperature vibration energy ($\sum_{\mathbf{q}}\hbar\omega_{\mathbf{q}}/2$), we find that the polaron energies at zero temperature coincide with the values of the adiabatic potential: $E_0(T=0) = J_0$.

As follows from (A19), the phonon wave function $\Phi_{\rm ph}(Q)$ with the displaced coordinates $\tilde{Q}$ at zero temperature is the phonon vacuum $|0_{\rm ph}\rangle$. Thus the phonon wave function $\Phi_{\rm ph}(Q) \equiv |\Phi_{\rm ph}\rangle$ can be expressed using the unitary operation acting on the phonon vacuum $|0_{\rm ph}\rangle$,

$$U = e^{-i\sum_{\mathbf{q}}Q_{\mathbf{q},0}P_{\mathbf{q}}}. \tag{A28}$$

This unitary operator of the displacement of the phonon coordinates can be equivalently re-written in terms of the second quantization operators,

$$U = e^{\sum_{\mathbf{q}}(f_{\mathbf{q}}b_{\mathbf{q}} - f_{\mathbf{q}}^* b_{\mathbf{q}}^+)}, \tag{A29}$$

where

$$f_{\mathbf{q}} = -\frac{1}{\sqrt{2}}Q_{\mathbf{q},0}^* = \frac{1}{\omega_{\mathbf{q}}^2}V_{\mathbf{q}}\rho_{\mathbf{q},0}. \tag{A30}$$

We can see that the unitary transformation (A29) is the same as that given by formula (9). Moreover, the adiabatic potential J_0 given by (A23) coincides with the polaron ground-state energy (18) when setting $\omega_{\mathbf{q}} = 1$. This shows the equivalence of the strong-coupling ansatz described in Sec. II to the rigorous strong-coupling scheme based on the adiabatic approximation. This scheme is asymptotically exact in the strong-coupling limit and was used for the numerically accurate calculation of the strong-coupling polaron energy in Ref. 31. In the present work, we use the strong-coupling polaron energies and wave functions within different approximations: within the Landau-Pekar (LP) approach[25] and within the approach of Ref. 31.

For the calculation of the optical conductivity, we use the set of the Franck-Condon (FC) excited states of the electron in the basis corresponding to the spherical symmetry of the system: $|\psi_{n,l,m}\rangle = R_{l,n}(r)Y_{l,m}(\theta,\varphi)$, where $R_{l,n}(r)$ is a radial wave function, and $Y_{l,m}(\theta,\varphi)$ is a spherical harmonic. In these notations, the ground-state wave function is $|\psi_0\rangle \equiv |\psi_{1,0,0}\rangle$. The FC states are defined as the eigenfunctions of the Hamiltonian (A11) with a potential $V_a(r)$ corresponding to a "frozen" lattice configuration for the ground state.

APPENDIX B: CORRELATION FUNCTION WITHIN THE ADIABATIC APPROXIMATION

The dipole-dipole correlation function $f_{zz}(t)$ given by (25) is further simplified within the adiabatic approximation and by using the selection rules for the dipole transition matrix elements and the symmetry properties of the polaron Hamiltonian.

First, within the adiabatic approximation, as discussed above, we find that

$$\langle\psi_0|S^+(t)|\psi_{n,l,m}\rangle \approx \delta_{n,1}\delta_{l,0}\delta_{m,0}\langle\psi_0|S^+(t)|\psi_0\rangle. \tag{B1}$$

Moreover, because the ground state ψ_0 is nondegenerate, within the same approximation, the averages $\langle\psi_0|W^n|\psi_0\rangle = 0$ for any $n \geqslant 1$, so that $\langle\psi_0|S^+(t)|\psi_0\rangle \approx 1$.

Therefore the correlation function (25) takes the form

$$\begin{aligned}f_{zz}(t) = \sum_{\substack{n',l',m',\\ n'',l'',m''}}&\langle\psi_0|z|\psi_{n'',l'',m''}\rangle\langle\psi_{n',l',m'}|z|\psi_0\rangle e^{it(E_0 - E_{n'',l''})} \\ &\times\langle 0_{\rm ph}|\langle\psi_{n'',l'',m''}|S(t)|\psi_{n',l',m'}\rangle|0_{\rm ph}\rangle.\end{aligned} \tag{B2}$$

As long as we deal with the wave functions in the spherical basis, we can use the selection rules for the dipole

transitions:

$$\langle\psi_0|z|\psi_{n'',l'',m''}\rangle = \delta_{l'',1}\delta_{m'',0}\langle\psi_0|z|\psi_{n'',1,0}\rangle, \tag{B3}$$

$$\langle\psi_{n',l',m'}|z|\psi_0\rangle = \delta_{l',1}\delta_{m',0}\langle\psi_{n',1,0}|z|\psi_0\rangle. \tag{B4}$$

Thus the correlation function is simplified:

$$f_{zz}(t) = \sum_{n',n}\langle\psi_0|z|\psi_{n,1,0}\rangle\langle\psi_{n',1,0}|z|\psi_0\rangle e^{it(E_0-E_{n,1})} \times \langle 0_{\rm ph}|\langle\psi_{n,1,0}|S(t)|\psi_{n',1,0}\rangle|0_{\rm ph}\rangle. \tag{B5}$$

A question can appear whether the adiabatic approximation works well for physically reasonable finite α. Certainly, the nonadiabatic corrections may be not small even for relatively large α, and diminish only in the limit $\alpha \to \infty$. However, we consider here only the trends of the optical conductivity in the limit of strong coupling and hence neglect the terms beyond the adiabatic approximation. Therefore, in the same approximation, we neglect in (B6) the matrix elements for $n' \neq n$. Therefore we approximate the correlation function (B5) by the expression

$$f_{zz}(t) \approx \sum_n D_n e^{-i\Omega_{n,0}t}\langle\psi_{n,1,0}|\langle 0_{\rm ph}| \times {\rm T}\exp\left[-i\int_0^t ds\, W(s)\right]|0_{\rm ph}\rangle|\psi_{n,1,0}\rangle \tag{B6}$$

with the squared matrix element of the dipole transition

$$D_n \equiv |\langle\psi_0|z|\psi_{n,1,0}\rangle|^2 = \frac{1}{3}\left(\int_0^\infty R_{n,1}(r)R_{0,0}(r)r^3dr\right)^2, \tag{B7}$$

and the FC transition frequencies

$$\Omega_{n,0} \equiv E_{n,1} - E_0. \tag{B8}$$

Further on, the interaction Hamiltonian is expressed in terms of the complex phonon coordinates $Q_{\mathbf{k}}$:

$$W = \sqrt{2}\sum_{\mathbf{k}} W_{\mathbf{k}}Q_{\mathbf{k}}, \quad Q_{\mathbf{k}} = \frac{b_{\mathbf{k}} + b^+_{-\mathbf{k}}}{\sqrt{2}}. \tag{B9}$$

Here, we use the spherical-wave basis for phonon modes:

$$\varphi_{k,l,m}(\mathbf{r}) \equiv (-1)^{\frac{m-|m|}{2}}\phi_{k,l}(r)\,Y_{l,m}(\theta,\varphi), \tag{B10}$$

where the radial part of the basis function is expressed through the spherical Bessel function $j_l(kr)$:

$$\phi_{k,l}(r) = \left(\frac{2}{R}\right)^{1/2} k\, j_l(kr), \quad R = \left(\frac{3V}{4\pi}\right)^{1/3}. \tag{B11}$$

The factor $(-1)^{\frac{m-|m|}{2}}$ is chosen in order to fulfill the symmetry property

$$\varphi^*_{k,l,m}(\mathbf{r}) = \varphi_{k,l,-m}(\mathbf{r}).$$

In the spherical-wave basis, the interaction Hamiltonian is

$$W = \sqrt{2}\sum_{k,l,m} W_{k,l,m}Q_{k,l,m}, \tag{B12}$$

with the complex phonon coordinates

$$Q_{k,l,m} = \frac{b_{k,l,m} + b^+_{k,l,-m}}{\sqrt{2}} \tag{B13}$$

and with the interaction amplitudes

$$W_{k,l,m} = \frac{\sqrt{2\sqrt{2}\pi\alpha}}{k}(\varphi_{k,l,m}(\mathbf{r}) - \rho_{k,l,m}), \quad \rho_{k,l,m} \equiv \langle\psi_0|\varphi_{k,l,m}|\psi_0\rangle. \tag{B14}$$

The dipole-dipole correlation function (B6) is then

$$f_{zz}(t) = \sum_n D_n e^{-i\Omega_{n,0}t}\langle\psi_{n,1,0}|\langle 0_{\rm ph}| \times {\rm T}\exp\left[-i\sqrt{2}\int_0^t ds\sum_{k,l,m} W_{k,l,m}(s)Q_{k,l,m}(s)\right] \times |0_{\rm ph}\rangle|\psi_{n,1,0}\rangle. \tag{B15}$$

After the averaging with the phonon wave function, the resulting evolution operator

$$S_e(t) \equiv \langle 0_{\rm ph}|{\rm T}\exp\left[-i\sqrt{2}\int_0^t ds\sum_{k,l,m} W_{k,l,m}(s)Q_{k,l,m}(s)\right]|0_{\rm ph}\rangle \tag{B16}$$

is a scalar of the rotation group. Therefore we can replace the diagonal matrix element of the T exponent in (B15) with the trace

$$f_{zz}(t) = \frac{1}{3}\sum_n D_n e^{-i\Omega_{n,0}t}\sum_{m=-1}^{1}\langle\psi_{n,1,m}|S_e(t)|\psi_{n,1,m}\rangle. \tag{B17}$$

The operators $W_{k,l,m}(s)$ in (B15) are equivalent to the $(2l+1)$-dimensional matrices $\mathbb{W}^{(n)}_{k,l,m}$ determined in the basis of the level (n,l). The matrix elements of these matrices are

$$\left(\mathbb{W}^{(n)}_{k,l,m}\right)_{m_1,m_2} = \langle\psi_{n,1,m_1}|W_{k,l,m}|\psi_{n,1,m_2}\rangle. \tag{B18}$$

In these notations, $f_{zz}(t)$ given by (B15) can be written down as

$$f_{zz}(t) = \frac{1}{3}\sum_n D_n e^{-i\Omega_{n,0}t}\sum_{m=-1}^{1}\langle 0_{\rm ph}| \times \left({\rm T}\exp\left[-i\int_0^t ds\,\mathbb{W}^{(n)}(s)\right]\right)_{m,m}|0_{\rm ph}\rangle = \frac{1}{3}\sum_n D_n e^{-i\Omega_{n,0}t}\langle 0_{\rm ph}| \times {\rm Tr}\left({\rm T}\exp\left[-i\int_0^t ds\,\mathbb{W}^{(n)}(s)\right]\right)|0_{\rm ph}\rangle, \tag{B19}$$

where $\mathbb{W}^{(n)}$ is the matrix electron-phonon interaction Hamiltonian expressed through the phonon complex coordinates in the spherical-wave representation as follows:

$$\mathbb{W}^{(n)} = \sqrt{2}\sum_{k,l,m}\mathbb{W}^{(n)}_{k,l,m}Q_{k,l,m}. \tag{B20}$$

Here, $\mathbb{W}^{(n)}_{k,l,m}$ is a (3×3) matrix in a basis of a level $(n,l)_{l=1}$ of the Hamiltonian $\tilde{H}_0$. As a result, we obtain the following expression for the polaron optical conductivity (4) with (B19):

$$\mathrm{Re}\,\sigma(\omega) = \frac{\omega}{6}\sum_n D_n \int_{-\infty}^{\infty} e^{i(\omega-\Omega_{n,0})t} \times \langle 0_{\mathrm{ph}}|\,\mathrm{Tr}\left(\mathrm{T}\exp\left[-i\int_0^t ds\,\mathbb{W}^{(n)}(s)\right]\right)|0_{\mathrm{ph}}\rangle dt. \tag{B21}$$

APPENDIX C: EFFECTIVE PHONON MODES

In order to perform the averaging in Eq. (32) analytically, we introduce the effective phonon modes $Q_{0,0}$ and $Q_{2,m}$ similarly to Ref. 30. The Hamiltonian $\mathbb{W}^{(n)}$ in terms of these effective phonon modes is expressed as

$$\mathbb{W}^{(n)} = \sqrt{2}\sum_{l,m}\tilde{\mathbb{W}}^{(n)}_{l,m}Q_{l,m}, \tag{C1}$$

where the matrices $\tilde{\mathbb{W}}^{(n)}_{l,m}$ (depending on the vibration coordinates $Q_{l,m}$) are explicitly given by the expressions (cf. Ref. 30)

$$\mathbb{W}^{(n)} = a_0^{(n)}\mathbb{I}\,Q_{0,0} + a_2^{(n)}\sum_{m=-2}^{2}\mathbb{B}_m Q_{2,m} \tag{C2}$$

with the matrices $\mathbb{B}_j$

$$\mathbb{B}_0 = \frac{1}{2\sqrt{5\pi}}\begin{pmatrix}-1&0&0\\0&2&0\\0&0&-1\end{pmatrix}, \tag{C3}$$

$$\mathbb{B}_1 = \mathbb{B}^+_{-1} = \frac{1}{2}\sqrt{\frac{3}{5\pi}}\begin{pmatrix}0&0&0\\-1&0&0\\0&1&0\end{pmatrix}, \tag{C4}$$

$$\mathbb{B}_2 = \mathbb{B}^+_{-2} = \sqrt{\frac{3}{10\pi}}\begin{pmatrix}0&0&0\\0&0&0\\-1&0&0\end{pmatrix}. \tag{C5}$$

The coefficients $a_0^{(n)}$ and $a_2^{(n)}$ in Eq. (C2) are

$$a_0^{(n)} = \left[\sqrt{2}\alpha\sum_k\frac{1}{k^2}(\langle\phi_{k,0}\rangle_{n,1} - \langle\phi_{k,0}\rangle_{0,0})^2\right]^{1/2}, \tag{C6}$$

$$a_2^{(n)} = \left(4\sqrt{2}\pi\alpha\sum_k\frac{1}{k^2}\langle\phi_{k,2}\rangle^2_{n,1}\right)^{1/2}. \tag{C7}$$

Here, $\phi_{k,l}$ is the radial part of the basis function expressed through the spherical Bessel function $j_l(kr)$:

$$\phi_{k,l}(r) = \left(\frac{2}{R}\right)^{1/2} k\,j_l(kr), \quad R = \left(\frac{3V}{4\pi}\right)^{1/3}, \tag{C8}$$

V is the volume of the crystal, and $\langle f(r)\rangle_{n,l}$ is the average

$$\langle f(r)\rangle_{n,l} = \int_0^\infty f(r)\,R^2_{n,l}(r)\,r^2 dr. \tag{C9}$$

The normalization of the phonon wave functions corresponds to the condition

$$\int_0^R \phi_{k,l}(r)\phi_{k',l}(r)r^2 dr = \delta_{k,k'}. \tag{C10}$$

After the straightforward calculation using (C10), we express the coefficients $a_0^{(n)}$ and $a_2^{(n)}$ through the integrals with the radial wave functions

$$a_0^{(n)} = \left\{2\sqrt{2}\alpha\int_0^\infty dr\int_0^r dr'\,r(r')^2\left[R^2_{n,1}(r) - R^2_{0,0}(r)\right] \times\left[R^2_{n,1}(r') - R^2_{0,0}(r')\right]\right\}^{1/2}, \tag{C11}$$

$$a_2^{(n)} = \left[\frac{8\sqrt{2}\pi\alpha}{5}\int_0^\infty dr\int_0^r dr'\frac{(r')^4}{r}R^2_{n,1}(r)R^2_{n,1}(r')\right]^{1/2}. \tag{C12}$$

1. Exact averaging

Let us substitute the matrix interaction Hamiltonian (C2) to the dipole-dipole correlation function (32), what gives us the result

$$f_{zz}(t) = \frac{1}{3}\sum_n D_n e^{-i\Omega_{n,0}t}\langle 0_{\mathrm{ph}}|\exp\left(-ita_0^{(n)}Q_0\right) \times \mathrm{Tr}\exp\left(-it\frac{a_2^{(n)}}{2\sqrt{5\pi}}\mathbb{V}(Q_2)\right)|0_{\mathrm{ph}}\rangle. \tag{C13}$$

Here, we use the matrix depending on the phonon coordinates,

$$\mathbb{V}(Q_2) \equiv 2\sqrt{5\pi}\sum_{m=-2}^{2}\mathbb{B}_m Q_{2m}, \tag{C14}$$

whose explicit form is

$$\mathbb{V}(Q_2) = \begin{pmatrix}-Q_{2,0} & -\sqrt{3}Q_{2,-1} & -\sqrt{6}Q_{2,-2}\\ -\sqrt{3}Q_{2,1} & 2Q_{2,0} & \sqrt{3}Q_{2,-1}\\ -\sqrt{6}Q_{2,2} & \sqrt{3}Q_{2,1} & -Q_{2,0}\end{pmatrix}. \tag{C15}$$

The matrix $\mathbb{V}(Q_2)$ is analytically diagonalized. The equation for the eigenvectors $|\chi(Q_2)\rangle$ and eigenvalues $\lambda(Q_2)$ of $\mathbb{V}(Q_2)$ is

$$\mathbb{V}(Q_2)\,|\chi(Q_2)\rangle = \lambda(Q_2)\,|\chi(Q_2)\rangle. \tag{C16}$$

The eigenvalues are found from the equation

$$\det(\mathbb{V}(Q_2) - \lambda(Q_2)\mathbb{I}) = 0. \tag{C17}$$

We make the transformation to the real phonon coordinates,

$$Q_{2,0} \equiv x_0, \quad Q_{2,m} \equiv \frac{x_m + iy_m}{\sqrt{2}}, \quad Q_{2,-m} = Q^*_{2,m} = \frac{x_m - iy_m}{\sqrt{2}}.$$

Five variables x_0, x_1, x_2, y_1, y_2 are the independent real phonon coordinates. The left-hand side of (C17) is expressed in terms

of these coordinates as

$$\det\left(\mathbb{V}(Q_2)-\lambda(Q_2)\,\mathbb{I}\right)=-\lambda^3+3p\lambda+2q \tag{C18}$$

with the coefficients

$$\begin{aligned}p&=x_0^2+x_1^2+x_2^2+y_1^2+y_2^2,\\ q&=x_0^3+\frac{3}{2}x_0\left(x_1^2+y_1^2\right)+\frac{3\sqrt{3}}{2}x_2\left(x_1^2-y_1^2\right)\\ &\quad-3x_0\left(x_2^2+y_2^2\right)+3\sqrt{3}x_1y_1y_2.\end{aligned}$$

So, we have the cubic equation for λ:

$$\lambda^3-3p\lambda-2q=0. \tag{C19}$$

Because the matrix $\mathbb{V}(Q_2)$ is Hermitian, all its eigenvalues are real. Therefore $\frac{|q|}{p^{3/2}}\leqslant 1$ [otherwise, $\sin(3\varphi)$ is not real]. Now, we have three explicit eigenvalues:

$$\begin{aligned}\lambda_1(Q_2)&=2\sqrt{p}\sin\left[\frac{\pi}{3}+\frac{1}{3}\arcsin\left(\frac{q}{p^{3/2}}\right)\right],\\ \lambda_2(Q_2)&=-2\sqrt{p}\sin\left[\frac{1}{3}\arcsin\left(\frac{q}{p^{3/2}}\right)\right],\\ \lambda_3(Q_2)&=-2\sqrt{p}\sin\left[\frac{\pi}{3}-\frac{1}{3}\arcsin\left(\frac{q}{p^{3/2}}\right)\right].\end{aligned} \tag{C20}$$

The trace in (C13) is invariant with respect to the choice of the basis. Consequently, after the diagonalization, $f_{zz}(t)$ takes the form

$$f_{zz}(t)=\frac{1}{3}\sum_n D_n e^{-i\Omega_{n,0}t}\sum_{j=1}^{3}\langle 0_{\rm ph}|\exp\left(-it\left[a_0^{(n)}Q_0+\frac{a_2^{(n)}}{2\sqrt{5\pi}}\lambda_j(Q_2)\right]\right)|0_{\rm ph}\rangle. \tag{C21}$$

After inserting $f_{zz}(t)$ given by (C21) into (4), the integration over time gives the δ function multiplied by 2π, and we arrive at the result

$$\mathrm{Re}\,\sigma(\omega)=\frac{\pi\omega}{3}\sum_n D_n\sum_{j=1}^{3}\langle 0_{\rm ph}|\delta\left(\omega-\Omega_{n,0}-a_0^{(n)}Q_0-\frac{a_2^{(n)}}{2\sqrt{5\pi}}\lambda_j(Q_2)\right)|0_{\rm ph}\rangle. \tag{C22}$$

The ground-state wave function for the effective phonon modes is

$$|0_{\rm ph}\rangle\equiv\Phi_0(Q)=\Phi_0^{(0)}(Q_0)\,\Phi_0^{(2)}(Q_2). \tag{C23}$$

$\Phi_0^{(0)}(Q_0)$ is the one-oscillator ground-state wave function:

$$\Phi_0^{(0)}(Q_0)=\pi^{-1/4}\exp\left(-\frac{Q_0^2}{2}\right). \tag{C24}$$

The ground-state wave function of phonons with $l=2$ is

$$\Phi_0^{(2)}(Q_2)=\pi^{-5/4}\exp\left[-\frac{1}{2}\left(x_0^2+\sum_{m=1,2}\left(x_m^2+y_m^2\right)\right)\right]. \tag{C25}$$

The phonon ground-state wave function (C23) is then

$$\Phi_0(Q)=\frac{1}{\pi^{3/2}}\exp\left[-\frac{1}{2}\left(x_0^2+\sum_{m=1,2}\left(x_m^2+y_m^2\right)+Q_0^2\right)\right]. \tag{C26}$$

With these phonon wave functions, Eq. (C22) results in the following expression for the polaron optical conductivity

$$\begin{aligned}\mathrm{Re}\,\sigma(\omega)=&\frac{\omega}{3\pi^2}\sum_n\frac{D_n}{a_0^{(n)}}\int_{-\infty}^{\infty}dx_0\int_{-\infty}^{\infty}dx_1\int_{-\infty}^{\infty}dx_2\int_{-\infty}^{\infty}dy_1\int_{-\infty}^{\infty}dy_2\\ &\times\sum_{j=1}^{3}\exp\left\{-\frac{1}{2}\left[x_0^2+\sum_{m=1,2}\left(x_m^2+y_m^2\right)+\frac{\left(\omega-\Omega_{n,0}-\frac{a_2^{(n)}}{2\sqrt{5\pi}}\lambda_j(Q_2)\right)^2}{\left(a_0^{(n)}\right)^2}\right]\right\}.\end{aligned} \tag{C27}$$

2. Averaging accounting for the static Jahn-Teller effect

In order to perform the phonon averaging explicitly, we disentangle the exponent $\exp(-it\sqrt{2}\sum_{l,m}\tilde{\mathbb{W}}_{l,m}^{(n)}Q_{l,m})$ as follows:

$$\exp\left(-it\sqrt{2}\sum_{l,m}\tilde{\mathbb{W}}_{l,m}^{(n)}Q_{l,m}\right)=\exp\left(-it\sum_{l,m}\tilde{\mathbb{W}}_{l,-m}^{(n)}b_{l,m}^{+}\right)\mathrm{T}\exp\left(-i\int_0^t ds\sum_{l,m}e^{is\sum_{l',m'}\tilde{\mathbb{W}}_{l',-m'}^{(n)}b_{l',m'}^{+}}\tilde{\mathbb{W}}_{l,m}^{(n)}b_{l,m}e^{-is\sum_{l',m'}\tilde{\mathbb{W}}_{l',-m'}^{(n)}b_{l',m'}^{+}}\right). \tag{C28}$$

Neglecting noncommutation of matrices $\tilde{\mathbb{W}}^{(n)}_{l,m}$, we find that

$$\sum_{l,m} e^{is\sum_{l',m'}\tilde{\mathbb{W}}^{(n)}_{l',-m'}b^{+}_{l',m'}}\tilde{\mathbb{W}}^{(n)}_{l,m}b_{l,m}e^{-is\sum_{l',m'}\tilde{\mathbb{W}}^{(n)}_{l',-m'}b^{+}_{l',m'}} = \sum_{l,m}\tilde{\mathbb{W}}^{(n)}_{l,m}b_{l,m} - is\sum_{l,m}\tilde{\mathbb{W}}^{(n)}_{l,-m}\tilde{\mathbb{W}}^{(n)}_{l,m}. \quad \text{(C29)}$$

The sum $\sum_{l,m}\tilde{\mathbb{W}}^{(n)}_{l,-m}\tilde{\mathbb{W}}^{(n)}_{l,m}$ in the basis (l,m) for a definite n is proportional to the unity matrix. Therefore $\exp(-it\sqrt{2}\sum_{l,m}\tilde{\mathbb{W}}^{(n)}_{l,m}Q_{l,m})$ is

$$e^{-it\sqrt{2}\sum_{l,m}\tilde{\mathbb{W}}^{(n)}_{l,m}Q_{l,m}} = e^{-it\sum_{l,m}\tilde{\mathbb{W}}^{(n)}_{l,-m}b^{+}_{l,m}}e^{-it\sum_{l,m}\tilde{\mathbb{W}}^{(n)}_{l,m}b_{l,m}-\frac{t^2}{2}\sum_{l,m}\tilde{\mathbb{W}}^{(n)}_{l,-m}\tilde{\mathbb{W}}^{(n)}_{l,m}}, \quad \text{(C30)}$$

that gives us the result

$$\langle 0_{\rm ph}|e^{-it\sqrt{2}\sum_{l,m}\tilde{\mathbb{W}}^{(n)}_{l,m}Q_{l,m}}|0_{\rm ph}\rangle = e^{-\frac{t^2}{2}\sum_{l,m}\tilde{\mathbb{W}}^{(n)}_{l,-m}\tilde{\mathbb{W}}^{(n)}_{l,m}}. \quad \text{(C31)}$$

Using the explicit formulas for the matrices $\tilde{W}^{(n)}_{l,m}$, the matrix sum takes the form

$$\sum_{l,m}\tilde{\mathbb{W}}^{(n)}_{l,-m}\tilde{\mathbb{W}}^{(n)}_{l,m} = \omega^{(n)}_s\mathbb{I} \quad \text{(C32)}$$

with the parameter

$$\omega^{(n)}_s = \frac{1}{2}\left(a^{(n)}_0\right)^2 + \frac{1}{4\pi}\left(a^{(n)}_2\right)^2. \quad \text{(C33)}$$

Using (C32), the optical conductivity (32) is transformed to the expression

$$\mathrm{Re}\,\sigma(\omega) = \omega\sum_n\sqrt{\frac{\pi}{2\omega^{(n)}_s}}D_n\exp\left[-\frac{(\omega-\Omega_{n,0})^2}{2\omega^{(n)}_s}\right]. \quad \text{(C34)}$$

*On leave from Department of Theoretical Physics, State University of Moldova, str. A. Mateevici 60, MD-2009 Kishinev, Republic of Moldova.

†Also at Technische Universiteit Eindhoven, P.O. Box 513, 5600 MB Eindhoven, The Netherlands.

[1] A. S. Alexandrov and J. T. Devreese, *Advances in Polaron Physics* (Springer, Berlin, 2010).

[2] S. Lupi, P. Maselli, M. Capizzi, P. Calvani, P. Giura, and P. Roy, Phys. Rev. Lett. **83**, 4852 (1999).

[3] F. Gervais, J. L. Servoin, A. Baratoff, J. G. Bednorz, and G. Binnig, Phys. Rev. B **47**, 8187 (1993).

[4] D. M. Eagles, M. Georgiev, and P. C. Petrova, Phys. Rev. B **54**, 22 (1996).

[5] Chen Ang, Zhi Yu, Zhi Jing, P. Lunkenheimer, and A. Loidl, Phys. Rev. B **61**, 3922 (2000).

[6] C. Z. Bi, J. Y. Ma, J. Yan, X. Fang, B. R. Zhao, D. Z. Yao, and X. G. Qiu, J. Phys.: Condens. Matter **18**, 2553 (2006).

[7] J. L. M. van Mechelen, D. van der Marel, C. Grimaldi, A. B. Kuzmenko, N. P. Armitage, N. Reyren, H. Hagemann, and I. I. Mazin, Phys. Rev. Lett. **100**, 226403 (2008).

[8] V. Gurevich, I. Lang, and Yu. Firsov, Fiz. Tverd. Tela **4**, 1252 (1962) [Sov. Phys. Solid State **4**, 918 (1963)].

[9] J. Devreese, W. Huybrechts, and L. Lemmens, Phys. Status Solidi B **48**, 77 (1971).

[10] B. E. Sernelius, Phys. Rev. B **48**, 7043 (1993).

[11] E. Kartheuser, R. Evrard, and J. Devreese, Phys. Rev. Lett. **22**, 94 (1969).

[12] M. J. Goovaerts, J. M. De Sitter, and J. T. Devreese, Phys. Rev. B **7**, 2639 (1973).

[13] D. Emin, Phys. Rev. B **48**, 13691 (1993).

[14] E. N. Myasnikov, A. E. Myasnikova, and Z. P. Mastropas, Phys. Solid State **48**, 1046 (2006).

[15] S. I. Pekar, *Untersuchungen über die Elektronentheorie der Kristalle* (Akademie-Verlag, Berlin, 1954).

[16] R. Feynman, R. Hellwarth, C. Iddings, and P. Platzman, Phys. Rev. **127**, 1004 (1962).

[17] R. P. Feynman, Phys. Rev. **97**, 660 (1955).

[18] J. Devreese, J. De Sitter, and M. Goovaerts, Phys. Rev. B **5**, 2367 (1972).

[19] J. T. Devreese, in *Polarons in Ionic Crystals and Polar Semiconductors* (North-Holland, Amsterdam, 1972), pp. 83–159.

[20] A. S. Mishchenko, N. V. Prokof'ev, A. Sakamoto, and B. V. Svistunov, Phys. Rev. B **62**, 6317 (2000).

[21] A. S. Mishchenko, N. Nagaosa, N. V. Prokof'ev, A. Sakamoto, and B. V. Svistunov, Phys. Rev. Lett. **91**, 236401 (2003).

[22] G. L. Goodvin, A. S. Mishchenko, and M. Berciu, Phys. Rev. Lett. **107**, 076403 (2011).

[23] G. De Filippis, V. Cataudella, A. S. Mishchenko, and N. Nagaosa, Phys. Rev. B **85**, 094302 (2012).

[24] G. De Filippis, V. Cataudella, A. S. Mishchenko, C. A. Perroni, and J. T. Devreese, Phys. Rev. Lett. **96**, 136405 (2006).

[25] L. D. Landau and S. I. Pekar, Zh. Eksp. Teor. Fiz. **18**, 419 (1948) [Ukr. J. Phys. **53**, 71 (2008)].

[26] G. R. Allcock, in *Polarons and Excitons*, edited by C. G. Kuper and G. D. Whitfield (Oliver and Boyd, Edinburgh, 1963), pp. 45–70.

[27] Note that this reasoning concerns the transitions due to the electron-phonon interaction but is not related to the dipole transitions described by the matrix elements $\langle\psi_{n,l,m}|z|\psi_{n'',l'',m''}\rangle$.

[28] Yu. E. Perlin, Sov. Phys. Usp. **6**, 542 (1964).

[29] H. Jahn and E. Teller, Proc. R. Soc. London A **161**, 220 (1937).

[30] V. M. Fomin, V. N. Gladilin, J. T. Devreese, E. P. Pokatilov, S. N. Balaban, and S. N. Klimin, Phys. Rev. B **57**, 2415 (1998).

[31] S. J. Miyake, J. Phys. Soc. Jpn. **38**, 181 (1975); **41**, 747 (1976).

[32] H. Kleinert, *Path Integrals in Quantum Mechanics, Statistics, Polymer Physics, and Financial Markets*, 5th ed. (World Scientific, Singapore 2009).

[33] J. T. Devreese, L. F. Lemmens, and J. Van Royen, Phys. Rev. B **15**, 1212 (1977).

[34] H. Spohn, Phys. Rev. B **33**, 8906 (1986); Ann. Phys. **175**, 278 (1987).